Heliyon 9 (2023) e16945

Contents lists available at ScienceDirect

Heliyon

journal homepage: www.cell.com/heliyon

Manufacture of antibacterial carbon fiber-reinforced plastics (CFRP) using imine-based epoxy vitrimer for medical application

Wonbin Kim [a,1], Yong Min Kim [a,b,1], SeungHyeon Song [a,c], Eunjung Kim [a,b], Dong-Gyun Kim [d], Yong Chae Jung [a], Woong-Ryeol Yu [b], WonJin Na [a,**], Yong-Seok Choi [a,*]

[a] *Composites Materials Application Research Center, Korea Institute of Science and Technology, 92 Chudong-ro, Bongdong-eup, Wanju-gun, Jeonbuk, 55324, Republic of Korea*

[b] *Department of Material Science and Engineering and Research Institute of Advanced Materials (RIAM), Seoul National University, Seoul, 151-742, Republic of Korea*

[c] *Functional Soft Materials Laboratory, School of Chemical Engineering Jeonbuk National University, Beakje-dearo 567, Deokjin-gu, 54896, Jeonju, Republic of Korea*

[d] *Advanced Materials Division, Korea Research Institute of Chemical Technology, 141 Gajeong-ro, Yuseong-gu, Daejeon, 34114, Republic of Korea*

ARTICLE INFO

Keywords:
A. polymer-matrix composites (PMCs)
A. Theromosetting resin
B. Chemical properties
Vitrimer

ABSTRACT

An antibacterial carbon fiber-reinforced plastics (CFRP) was manufactured based on a vitrimer containing imine groups. A liquid curing agent was prepared to include an imine group in the matrix, and was synthesized without a simple mixing reaction and any purification process. The vitrimer used as the matrix for CFRP was prepared by reacting a commercial epoxy with a synthesized curing agent. The structural and thermal properties of the vitrimer were determined by Fourier transform-infrared spectroscopy (FT-IR), differential scanning calorimetry (DSC) and thermogravimetric analysis (TGA). In addition, the temperature-dependent behavior of the vitrimer was characterized by stress relaxation, reshaping, and shape memory experiments. The mechanical properties of composites fabricated using vitrimer were fully analyzed by tensile, flexural, short-beam strength, and Izod impact tests and had mechanical properties similar to reference material. Moreover, both the vitrimer and the vitrimer composites showed excellent antibacterial activity against *Staphylococcus aureus* and *Escherichia coil* due to the imine group inside the vitrimer. Therefore, vitrimer composites have potential for applications requiring antimicrobial properties, such as medical devices.

1. Introduction

Carbon fiber-reinforced plastics (CFRP) are of interest as a metal substitute to enable weight reduction because of their high strength and rigidity-to-weight ratio. In particular, the excellent physical properties of CFRP enable their utilization in mass transportation models, such as aircraft, automobiles, high-speed trains, and boats [1–3]. Applications to medical, energy and electronic

* Corresponding author. Korea Institute of Science and Technology, Republic of Korea.
** Corresponding author.
E-mail addresses: namossi@kist.re.kr (W. Na), choiys@kist.re.kr (Y.-S. Choi).
[1] These authors contributed equally to this work.

https://doi.org/10.1016/j.heliyon.2023.e16945
Received 18 November 2022; Received in revised form 30 May 2023; Accepted 1 June 2023
Available online 2 June 2023

materials are being studied following the introduction of antibacterial, electrical conductivity, and thermal conductivity properties to CFRP [4–7]. In particular, the medical application of CFRP is important for the improvement of human health and welfare. Due to the low X-ray transmittance of traditional metal-based medical devices for immobilization of the surgical site, X-ray scans often need to be repeated numerous times during a surgical procedure to provide complete information. However, due to the excellent X-ray transmittance of CFRP, complete data can be obtained with only one X-ray irradiation step, thereby minimizing exposure of the human body to X-rays [8]. Therefore, it is expected that the traditional material used for medical devices will be rapidly replaced by CFRP.

CFRP is generally manufactured using thermosetting resins as matrix materials because of their high mechanical and thermal stability, environmental resistance, and excellent interfacial properties (with carbon fibers). However, thermosetting materials have serious economic and physical drawbacks, such as yellowing and poor impact resistance, and their inability to reshape and recycle due to their crosslinked structures [9]. Therefore, research is underway to replace the thermosetting resin within a CFRP with a thermoplastic resin [10]. In particular, vitrimers, which have the properties of both thermosetting and thermoplastic resins, could serve as the ideal substitute for a thermosetting resin [11,12]. Therefore, vitrimer can be utilized to manufacture novel recyclable and reshapable CFRP. Some groups exploited the reprocessability of vitrimers to prepare thermoformable pultruded CFRP [13]. One group studied on efficient recycling of carbon fiber in CFPR through chemical degradation using covalent bond exchange reactions of the vitrimer [14].

The aforementioned vitrimer is a polymer that undergoes a crosslinking exchange reaction at a certain temperature, called the vitrimer transition temperature (T_v) [15,16]. Vitrimers are covalent adaptive networks (CANs) whose structures rearrange thermally via changes in bonding while the degree of crosslinking remains constant [17,18]. Therefore, although a CAN is a thermosetting material, it has the great advantage of being able to remain to reshape properties and reprocessability above T_v, similar to thermoplastic material, and can potentially be recycled. Additionally, vitrimers commonly exhibit shape memory properties due to their cross-linked structures, and there have been studies on vitrimer composites with shape memory capabilities [19,20]. Vitrimers can be prepared by introducing covalent bonds which undergo various exchange reactions, such as transesterification, transcarbonation, and transimination exchange reactions [15,17,18]. The imine bond is particularly suitable for a material requiring excellent physical properties, and the transimination exchange reaction proceeds at low temperatures without a catalyst. The imine bond can be readily synthesized via the reaction of a primary amine and an aldehyde. Furthermore, the antibacterial properties of the imine group suggest the potential application of vitrimers as water treatment, medical, and coating materials [21–23]. Therefore, it can be said that manufacturing CFRP using a material containing an imine group with antibacterial properties is important in terms of expanding the application potential of CFRP to various fields. In particular, the imine group, which exhibits antibacterial properties upon contact, which is not a leaching type, continuously maintains antibacterial properties, and can maintain antibacterial properties semi-permanently via continuous cleaning [24].

Herein, we report the preparation of antibacterial CFRP using imine-based epoxy vitrimer. First, to prepare a vitrimer having antibacterial properties, an Imine-Amine (IA) curing agent containing imine groups was synthesized according to a simple mixing–heating reaction without any purification process. An epoxy vitrimer having a crosslinked structure was synthesized through the reaction of the IA with a commercial epoxy without any solvent, and imine exchange proceeded successfully above T_v. CFRP was manufactured by impregnating carbon fibers with an imine curing agent (IA) and commercial epoxy. All processes were carried out under environmentally friendly conditions in the absence of solvent. The thermal, mechanical, and malleability of vitrimers were determined by thermogravimetric analysis (TGA), differential scanning calorimetry (DSC), dynamic mechanical analysis (DMA), and universal testing machine (UTM). In addition, chemical and physical stability, reshaping, and antibacterial properties were measured under various conditions.

2. Experimental

2.1. Materials

Terephthalaldehyde and tetrabutylammonium tribromide were purchased from Sigma–Aldrich (USA). Jeffamine D-230 (n ~2.5) amine curing agent was purchased from New Seoul Chemical (Korea). Epoxy resin (YD115) was purchased from Kukdo Chemical (China). Epichlorohydrin was purchased from Tokyo Chemical Industry (Japan). Sodium hydroxide (50% solution) was purchased from Samchun Chemicals (Korea). Carbon fiber (T300) was purchased from Toray. Unless otherwise stated, all reagents were purchased from commercial suppliers and used as-received.

2.1.1. Synthesis of jeffamine D-230 (n ~2.5)/epoxy resin (YD115)

Curing agent (Jeffamine D-230; n ~2.5; 1.0 equiv., 40 mmol, 5 g) and epoxy resin (YD115; 1.0 equiv., 16 g) were mixed in a 100 mL vial at an equivalent ratio of 1:1, and the solution was degassed under vacuum for 1 h. The degassed liquid was then poured into dog-bone- and square-shaped molds and cured in an oven at 130 °C for 6 h.

2.1.2. Synthesis of imine-amine hardener

Terephthalaldehyde (60 g, 447 mmol) and Jeffamine D-230 (206 g, 895 mmol) were added to a two-necked round-bottomed flask equipped with a reflux condenser at a 1:2 M ratio. No solvent was added. The mixture was stirred at 65 °C for 24 h under an N_2 atmosphere to obtain the IA product (250 g, 558 g/mol), which was used without further purification.

2.1.3. Synthesis of vitrimer

This reaction was carried out under the same conditions as the reaction of Jeffamine D-230 (n ~2.5) with epoxy resin (YD115). IA hardener (1.0 equiv., 36 mmol, 5 g) and epoxy resin (YD115; 1.0 equiv., 72 mmol, 7 g) were thoroughly mixed in a 100 mL vial at an equivalent ratio of 1:1. After degassing under vacuum, the liquid was poured into dog-bone- and square-shaped molds and allowed to react in a vacuum oven at 130 °C for 6 h.

2.1.4. Fabrication of carbon fiber-reinforced plastics (CFRP)

The CFRPs were fabricated using IA, YD115, and T300 as the hardener, epoxy, and carbon fiber, respectively. Jeffamine D-230 (D230, Huntsman Chemicals Co., USA) was used as the commercial hardener for the reference material. The mixture of bisphenol-A epoxy resin (YD-115; Kukdo Chemical Co., Korea) and hardener was degassed for more than 1 h under vacuum. The degassed resin was impregnated into plain-woven carbon fiber fabric (C-120 fabric from Minhu Composites, Korea, made from Toray T-300 fiber of tow size 3 K) by hand lay-up. The impregnated fabric was placed in an aluminum mold and compressed at 5 MPa (120 °C) for 1 h to produce a composites plate (Fig. S6). The thickness of test specimens was varied according to the requirement of each test method by controlling the number of plies. Specifically, the tensile test specimens were 2-mm thick (12 plies), and the three-point bending test, short-beam strength test (for interlaminar shear strength [ILSS] measurement), and Izod impact test specimens were 3.5-mm thick (20 plies). For the antibacterial test, 1.5-mm-thick specimens were fabricated from eight plies. The fiber volume fraction in the composite was calculated through density measurements. All CFRPs exhibited a fiber fraction between 45.0 and 46.0 vol%.

2.2. Characterization

2.2.1. Vitrimers

Proton nuclear magnetic resonance (^{1}H NMR) spectra of IA were measured using a 600 MHz Premium COMPACT NMR instrument (Agilent, USA) with chloroform-*d* as the solvent. Fourier transform-infrared (FT-IR) spectra of vitrimer samples were acquired using a Nicolet iS10 instrument operating in attenuated total reflectance (ATR) mode (Thermo Fisher Scientific, USA); 64 scans were performed from 4000 to 500 cm^{-1}. The DSC thermograms were obtained using a DSC25 instrument (TA Instruments, USA). Samples (~5–10 mg) were loaded in standard aluminum DSC pans and heated from 40 °C to 250 °C at a rate of 10 °C/min under an N_2 atmosphere. TGA plots were obtained using a TGA55 instrument (TA Instruments). The samples (~5–10 mg) were loaded in alumina TGA pans, and heated from 40 °C to 900 °C under an N_2 atmosphere at the rate of 10 °C/min. The mechanical properties were measured using a UTM (model 5567 A; Instron, USA) equipped with a 2-kN load cell according to the ASTM D638 standard. Dog-bone-shaped test specimens had dimensions (in mm) of 25 (length) × 10 (width) × 10 (neck length) × 3 (neck width) × 0.10 (thickness). Dynamic mechanical thermal analysis was conducted using a TA Instruments Q800 instrument to characterize the relaxation behavior of the vitrimer. Samples were strained at 2% at selected temperatures (120, 140, 160, 180, and 200 °C) and the stress relaxation behavior of the samples was then recorded. DMA was also conducted in the film tension mode with a 1 Hz frequency, 0.1% strain, and 0.1 N axial force for calculation of cross-linking density (ν_e) using rubber elasticity theory of Flory as below.

$$\nu_e = E' / 3RT \quad (1)$$

where E′, R, and T are the storage modulus, universal gas constant, and absolute temperature in the rubbery region, respectively. Shape memory cycle test of vitrimer was conducted by DMA Q800 with attached cryo accessory under controlled force mode. The antibacterial activity of the samples was measured according to the JIS Z 2801:2010 method.

2.2.2. Carbon fiber-reinforced plastics

Specimens for mechanical testing were prepared according to the relevant ASTM standards (Fig. S7). The tensile strength, bending strength, ILSS, and impact resistance of composites materials were measured. For the tensile test, the composites plate was cut into a piece of dimensions 180 × 18 mm^2 (ASTM D3039) and 40 × 18 mm^2 GFRP tabs were attached to both ends to form a specimen having a gauge length of 100 mm (Fig. S7a). These specimens were tested using an Instron 5985 UTM operating at a crosshead speed of 1 mm/min. A strain gauge was attached to the center of a specimen to measure strain. Three-point bending test specimens were cut into rectangular pieces of dimensions 140 × 14 mm^2 according to the ASTM D790 standard, and tested at 1.5 mm/min using an Instron 4464 UTM (Fig. S7b). The ILSS test specimens of dimensions 21 × 7 mm^2 were prepared according to the ASTM D2344 standard and tested at a crosshead speed of 1 mm/min (Fig. S7c). Izod impact test specimens having dimensions 63.5 × 12.7 mm^2 were prepared according to the ASTM D256 standard and a 2.54-mm deep, 45° notch was introduced using a notcher (model 898; Tinius Olsen, USA). Izod impact resistance was measured using a pendulum impact tester (IT 504; Tinius Olsen) (Fig. S7d).

3. Results and discussion

3.1. Synthesis of imine-containing vitrimer

The IA hardener was first synthesized from terephthalaldehyde and Jeffamine D230 (Jeffamine D230 [n = ~2.5]) in a mole ratio of 1:2 via a simple mixing and heating process in the absence of solvent and catalyst. Successful synthesis of the IA hardener was confirmed by ^{1}H- NMR (Fig. S1). The terephthalaldehyde peak at 10.13 ppm was upshifted to 8.30 ppm at reaction completion, indicating that all of the aldehyde groups in the terephthalaldehyde had reacted with the amine groups of Jeffamine D230. Since,

water, a by-product of the reaction of an aldehyde with an amine, was easily removed by evaporation in a vacuum, it is expected that IA can be easily applied industrially by scale-up. In addition, the imine groups formed via the chemical reaction of terephthalaldehyde with Jeffamine D230, were expected to impart both antibacterial and reshaping properties to the epoxy resin.

The vitrimer was prepared by traditional epoxy manufacturing methods, using YD115 as the epoxy and IA as the curing agent, in the absence of solvent (Fig. 1). The YD115 and IA were mixed at a 1:1 ratio (epoxy equivalents:active amine hydrogen equivalents) for complete crosslinking reaction. The mixture was cured in an oven at 130 °C for 6 h to form the vitrimer. A reference sample was also prepared under the same conditions, but YD115 was used as the epoxy and Jeffamine D230 as the curing agent. There was no exothermic peak at temperatures above 100 °C in the DSC thermogram of the samples, indicating that no residual epoxy was present, i.e., the reaction was complete (Fig. 2b). FT-IR analysis in ATR mode confirmed that a fully crosslinked vitrimer was prepared (Fig. S2). A peak corresponding to the N–C group resulting from the amine–epoxy reaction appeared at 1370 cm^{-1}. The imine peak (N═C stretching vibration) of the vitrimer observed at 1607 cm^{-1} was due to the reaction of the epoxy group with the amine group [25]. In addition, peaks corresponding to the primary amine groups of Jeffamine D230 and the epoxy group of YD115 were not observed, consistent with the amine-epoxy crosslinking reaction.

3.2. Characterization of vitrimer

3.2.1. Thermal and mechanical properties, and chemical stability

The thermal and mechanical properties of the vitrimer were analyzed in various ways. The vitrimer was decomposed around 300 °C (temperature at 5% weight loss, $T_{d\ 5\%}$) which is thermally stable according to TGA. Its thermal decomposition temperature was somewhat lower than that of the reference, which is related to crosslink density (Fig. 2a). The IA had a longer backbone than Jeffamine D230, In other words, although it contains a benzene ring with high thermal stability [26], which led to increases the distance between cross-linking points and affects the thermal properties of the vitrimer [27]. The vitrimer decomposed to form more char than the reference; this was due to the nitrogen group having flame-retardant properties, as reported previously [28–30]. The DSC data showed that the vitrimer had a relatively lower glass transition temperature (T_g; 55 °C compared with 68 °C for the reference) (Fig. 2b). The low cross-linking density ($\nu_e = 406$ mol m^{-3}, calculated with equation (1)) caused by IA, which has a relatively high molecular weight compared to D230, increases chain mobility and lowers the T_g (Fig. 3a) [31]. The average tensile strength of the vitrimer was 60.60 MPa, which is similar to that of the reference material (61.21 MPa) (Fig. 2c and Table S1). On the other hand, the tensile strain at break was 0.063 mm/mm, which is higher than that of reference (0.039 mm/mm) (Fig. 2c). Chemical stability was established by observing physical changes over time while the sample was immersed in various solvents, including organic solvents (Tetrahydrofuran (THF), Acetone, Ethanol, *N*,*N*-dimethylformamide (DMF)) and aqueous acid (1 M H_2SO_4). The vitrimer was stable to at least 96 h in each liquid; no deformation or weight loss was observed (Fig. S4). The chemical stability of the vitrimer toward organic solvents depended

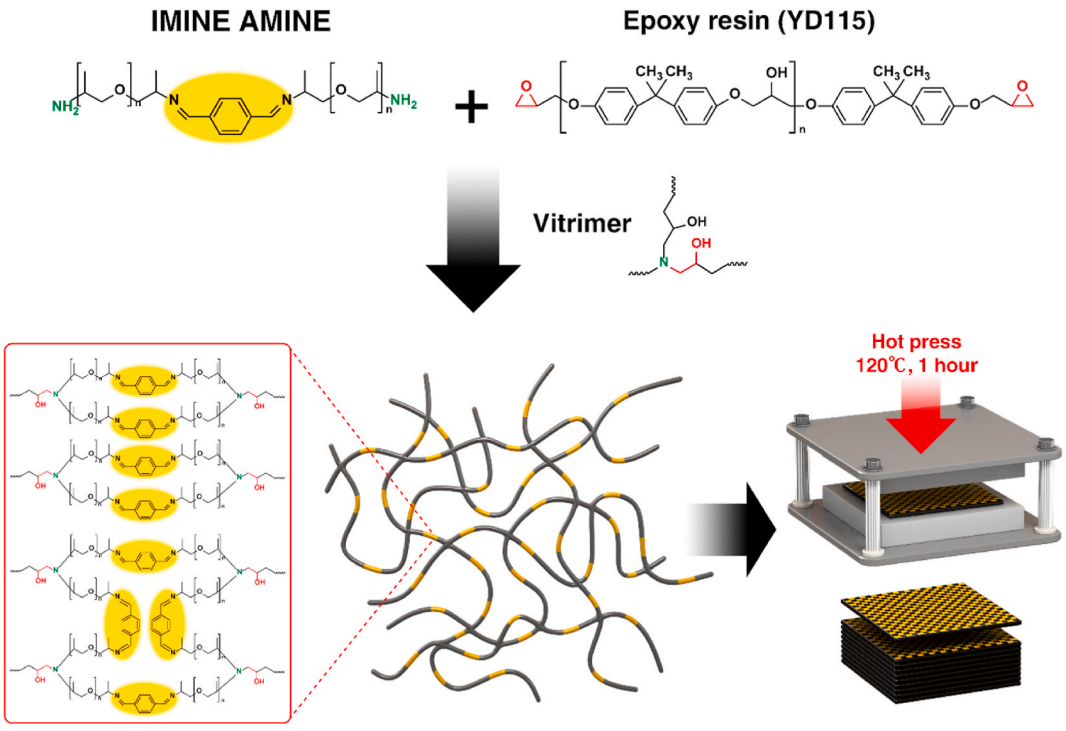

Fig. 1. Schematic illustration of synthesis of imine-containing vitrimer using Imine-Amine (IA) as the curing agent and YD115 as the epoxy in the absence of solvent.

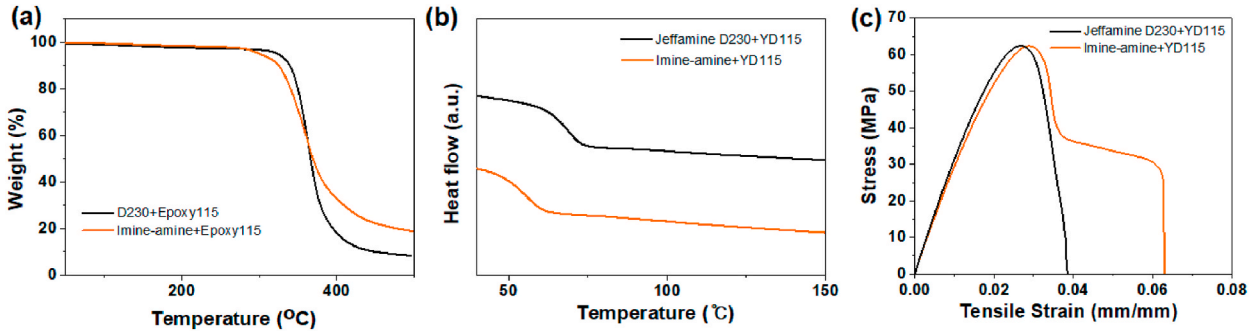

Fig. 2. The thermal and mechanical properties of the imine-containing vitrimer (IA + YD115) and reference (Jeffamine D230 +YD115) sample. (a) TGA curves; (b) DSC curves; and (c) The tensile stress-strain curves.

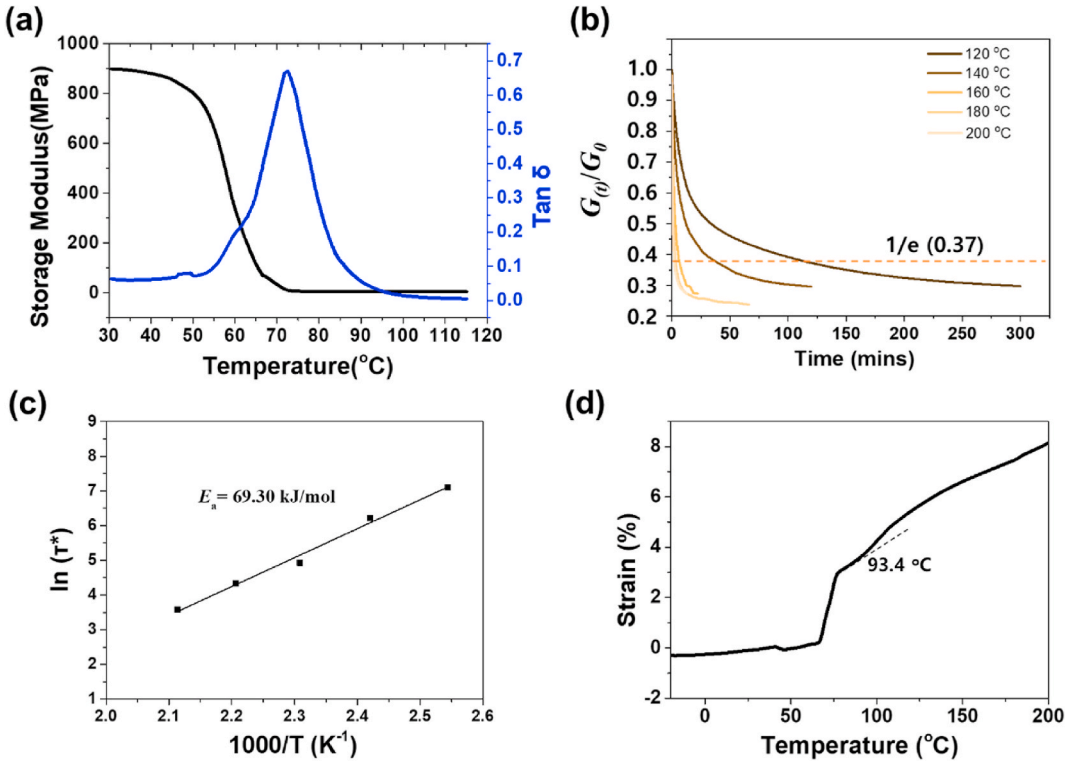

Fig. 3. (A) Plots of storage modulus and tanδ curves, (b) The stress relaxation curves over the range of 120 C–200 C and (c) Linear fitted curve based on the Arrhenius equation and calculated activation energy. (d) Temperature dependence of thermal expansion of vitrimer.

on the crosslinked structure formed by the amine-epoxy reaction, as expected. The vitrimer also showed good resistance to 1 M H_2SO_4, although it is well-known that an imine group is readily hydrolyzed under acidic conditions. Hydrolysis of the imine group inside the vitrimer was additionally confirmed in a mixed solvent of 1 M H_2SO_4 and THF (2:8 v/v) at 50 °C. A weight loss of 23.7 wt% occurred, complete decomposition did not proceed when vitrimer was immersed in a mixed solvent for 24 h (Fig. S9). This resistance may be due to polymeric fragments. The good stability of the vitrimer in aqueous acid was attributed to the location of the imine groups in the IA curing agent, as reported by Otsuka et al. [32]. According to Otsuka research, the moiety with dynamic covalent bonds is an important factor in the degradation efficiency of polymers. Vitrimer synthesized from epoxy with dynamic covalent bond form and drive more bond exchange reaction than its of diamine moieties with dynamic covalent bond. In other words, fewer dynamic covalent bonds in vitrimer lead to the formation of larger fragments during degradation. That is, the difference in fragments affects the resistance. The excellent chemical and acid stabilities of imine vitrimers suggest applications in extreme environments and medical materials.

3.2.2. Shape memory and reshaping properties

Viscoelastic behavior of the polymers is characterized by stress relaxation, shape memory, and reshaping test. The vitrimer

behavior was characterized by stress relaxation experiments carried out over the range of 120C–200C (Fig. 3b). The characteristic relaxation time is defined as that when the normalized relaxation modulus, $G_{(t)}/G_0$, is $1/e$ (37%) of the initial value. The relaxation time depend on temperature; it decreased with increasing temperature and was 7384 s at 120C and 135 s at 200C (Fig. 3b). The characteristic relaxation time (τ) and temperature (T) data were fitted to the Arrhenius equation (Fig. 3c), where the activation energy (E_a) is the slope of the relaxation time plotted as a function of temperature and R is the universal gas constant [33]. The obtained activation energy of imine bond exchange was calculated as 69.3 kJ/mol. The activation energy values of imine bond exchange were approximately range from 48 to 157 kJ/mol in previously studies, and our study has appropriate activation energy value [34]. Vitrimer behavior was activated by a dynamic exchange reaction of imine bonds with increasing temperature; the relaxation time steadily decreased due to the molecular rearrangement process. That is, the constant change in viscosity with temperature, which is a distinguishing characteristic of vitrimer behavior. The existence of T_v in the vitrimer was confirmed by dialotometry experiments. As shown in the strain-temperature curve (Fig. 3d), the slope of the sample remains constant from −20 C 200 C, as expected for a typical cross-linked network. With a further increase in temperature, an obvious increase in the thermal expansion coefficient is observed at about 93.4 C, which is due to thermally activated imine bond exchange reactions [35]. Shape memory vitrimer behavior was also confirmed. This is a property whereby a shape deformed by an external stimulus returns to its original shape [36]. The polymer chains move, and the soft segments become more flexible, at a temperature above T_g. Fig. 4a–c shows that the dog-bone-shaped vitrimer sample was bent and deformed into a U-shape by an external force applied at 60 C for 30 min, and that the shape was maintained as the temperature was decreased to room temperature and maintained for 1 h. With shape memory behavior, the polymer chain arrangement does not change and the specimen shape is temporarily maintained; it returns to its original shape, even in the absence of an external force, at temperatures above its T_g due to its elastic properties by covalently crosslinked network.

The vitrimer exhibits typical unidirectional double-shape memory behavior, even when evaluated by DMA (Fig. 4g). After stretching with a tensile stress of 0.20 MPa at 60C, lower the temperature to 20C and remove the stress to fix it. The temporarily fixed shape of the vitrimer returns to its original shape when heated to 60C. The vitrimer showed good fixation (R_f), although the shape recovery (R_r) decreased with repeated testing. The decrease in R_r can be attributed to the imine exchange reaction observed during the test. This reaction is initiated by an increase in temperature, leading to the weakening of the network structure within the elastomer. The decrease in R_r is a consequence of the reconfiguration of the samples caused by the imine exchange reaction, which in turn results in a reduction of the storage modulus necessary for shape recovery. In a related study, Huang et al. systematically analyzed the shape memory effect of TPU incorporating dissociative CAN, specifically by increasing the temperature [19]. The rise in temperature induces a weakening of the cross-linked network, which corresponds to the hard segment in the elastomer, leading to a decrease in R_r that aligns with our own findings. However, under conditions above the T_v, a vitrimer can fully deformed by chain exchange; this is called reshaping. Fig. 4d–e shows that the U-shape of the deformed vitrimer did not return to its original shape, and kept its form when an external force was applied at 140C for 24 h. This is attributed to dynamic covalent bonding of the vitrimer. The vitrimer underwent imine-imine (imine metathesis) bond exchange and constantly rearranged its molecular topology above the T_v, thereby maintaining its shape. The rearranged molecular structure enabled the deformed morphology to be maintained under continuous application of an external force and temperature. Reshaping via a simple process is a unique characteristic of vitrimer due to the exchange reaction between imine bonds.

3.3. Mechanical properties of CFRPs

Fig. 5 presents the tensile test results. Similar to ordinary CFRPs, the composites displayed a linear stress−strain response and brittle failure behavior. The stress−strain curves of the reference and vitrimer composites were similar (Fig. 5a). The slightly lower (4%) tensile strength of the vitrimer composites may be due to experimental variation, although the low standard deviation of the measurements (15 MPa) suggests mechanical property degradation (Fig. 5b). The effect of hardener structure on interfacial properties

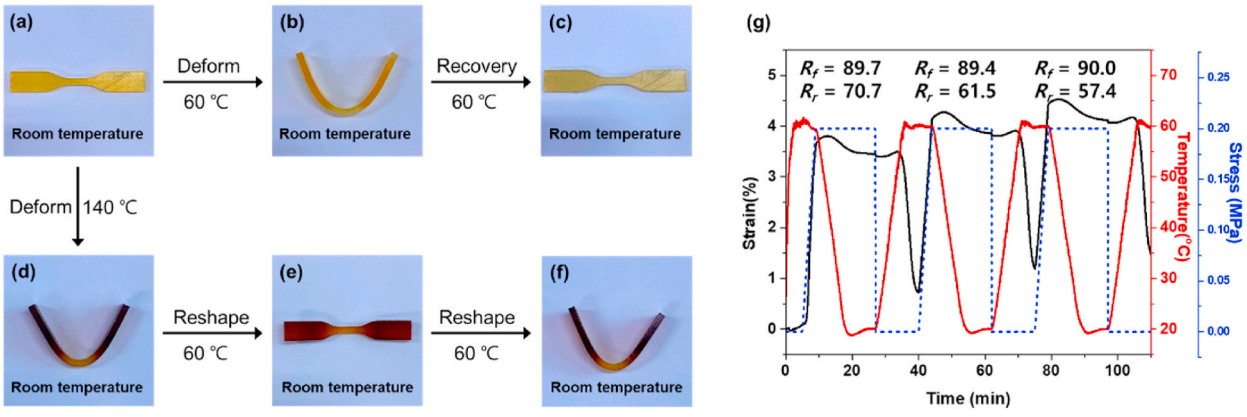

Fig. 4. Shape memory and reshaping photograph of the imine-containing vitrimer. (a–c) Shape memory of the vitrimer at temperatures above its T_g and (a-d, *d*-f) Reshaping of the vitrimer at temperatures above the T_v. (g) Consecutive shape memory cycles curves for vitrimer.

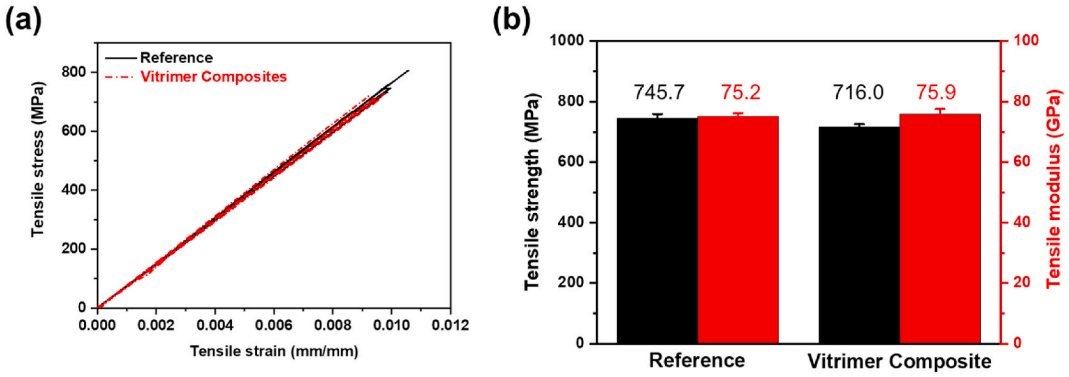

Fig. 5. (A) The stress-strain curves and (b) tensile properties of composites.

may contribute to degradation. Na et al. attributed 5–10% of the variation in tensile strength of a composites to interfacial properties [37,38]. When a fiber is broken under low stress, stress redistribution near the broken fiber can be affected by poor interfacial properties, thereby decreasing the total load-carrying capacity. However, since tensile properties are primarily determined by the fiber properties, the change in hardener did not cause a significant change in tensile properties within the epoxy resin system.

The effect of interfacial properties is more apparent in the flexural test results (Fig. 6). Unlike tensile strength, the flexural strength of the vitrimer composites decreased (by 21.55%) compared with the reference (Fig. 6b). They had the same initial modulus according to their stress−strain curves (Fig. 6a). However, the tangent modulus of the vitrimer composites decreased with increasing strain, showing slightly nonlinear behavior after 0.5% strain. In addition, at the ultimate flexural strength, the reference composites displayed brittle failure, i.e., a sudden decline in stress, while the vitrimer composites displayed ductile failure. Fiber-bundle fracture was evident at the lower surface of the reference composites specimen, while the vitrimer composites flexural specimen displayed interlaminar cracking near the upper surface (Fig. 6c). Wang et al. reported that the failure morphology of a composites is determined by the change of interlaminar shear stress with temperature [39]. Therefore, the yielding zone of the vitrimer composites is interpreted as a region of

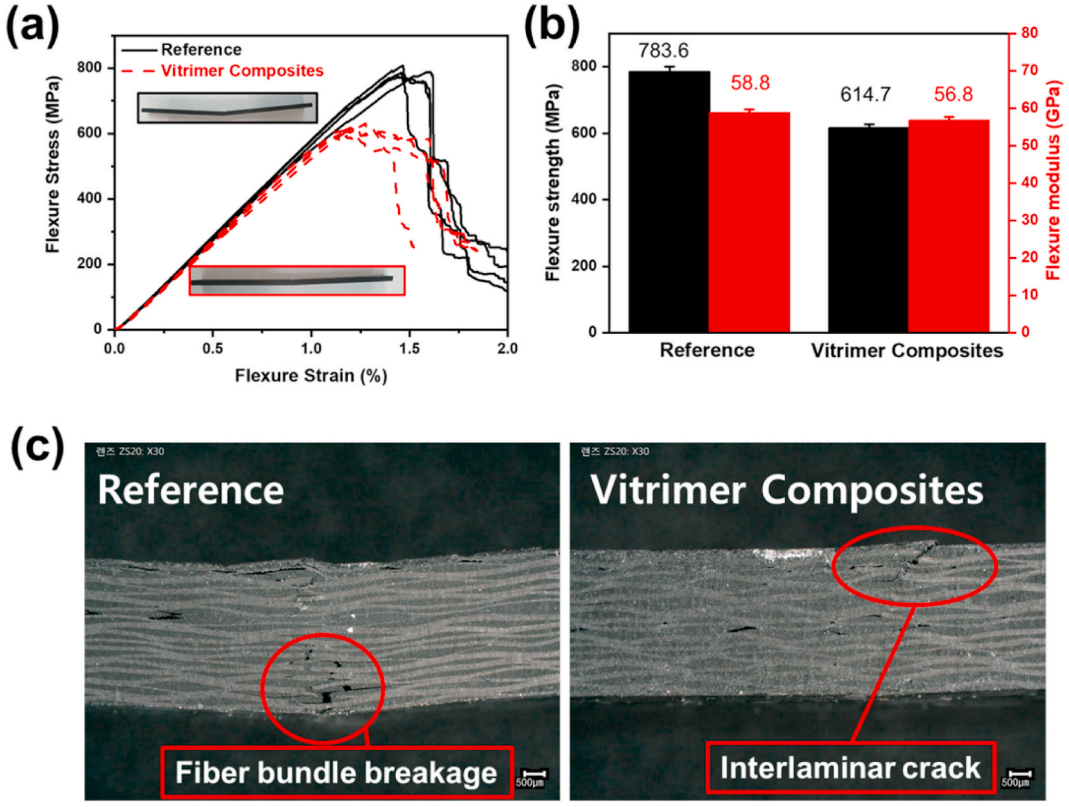

Fig. 6. (A) The flexural stress-strain curves; (b) flexural properties of composites; and (c) Failure morphology of reference and vitrimer composites.

relatively poorer interlaminar properties compared with the reference composites. The trends in short-beam strength and bending test results were in agreement, i.e., the ILSS of the vitrimer composites was lower by 10.47% (Fig. 7a). Partial interfacial separation occurred as bending proceeded, thereby reducing the tangent modulus, and delamination occurred above a particular stress value, resulting in yield behavior (Fig. 7b).

The chemical structures of the epoxy resins and hardeners affected the interfacial shear strength (IFSS) and ILSS of the products [40,41]. Bonding to carbon fiber involves hydrogen bonds between the –COOH and –OH groups on the carbon fiber surface, and the oxygen atoms of the epoxy group. Hydrogen bonding between nitrogen and oxygen was less extensive in the vitrimer composites than reference epoxy [42], and the interfacial bond strength was accordingly lower. The tensile properties of the composites material were more influenced by the properties of the carbon fiber than those of the matrix, but the bending strength and ILSS decreased due to reduced interfacial bonding. In Fig. 7b, the failure strain of the vitrimer composites is larger than that of the reference material. But the strain at which the modulus decrease (yielding point in homogeneous material) is less than that of reference material, indicating the effect of weak interfacial bonding.

The Izod impact test was used to assess interfacial bond strength. There was little difference (2.58%) in impact strength between the reference and vitrimer composites samples (Fig. S8). However, in-plane failure testing according to the Izod pendulum test revealed a significant difference in absorption energy due to the brittleness of the epoxy resin. Even in a woven composites having a low IFSS, cracks tend to propagate in the weaker weft direction and debonding is less likely [43,44]. Our results imply that the lower interfacial bond strength, but not the tensile properties and impact resistance, of the vitrimer composites was due to the curing agent.

3.4. Antibacterial properties

The antibacterial properties of resins and composites against both *Staphylococcus aureus* (*S. aureus*, Gram-positive) and *Escherichia coli* (*E. coli*, Gram-negative) were measured according to the JIS.Z.2801 method. The epoxy vitrimer showed good antibacterial activities against *S. aureus* and *E. coli* (84.9% and 67.9%, respectively) (Fig. 8). The antibacterial properties of vitrimers are likely attributable to the imine bond, as reported previously [45,46]. Although the antibacterial performance was slightly lower compared with that of the bare resin, the CFRP prepared using the epoxy vitrimer also showed good antibacterial effects against *S. aureus* and *E. coli* (71.5% and 38.9%, respectively).

The different antibacterial behaviors of CFRP and resin may be due to the extent of contact between the resin and bacteria [47,48]. Non-release-type contact antibacterial materials show a positive correlation between surface area and antibacterial properties. Since CFRP, which is composed of resin and carbon fiber, has a smaller exposed resin surface than bare resin, contact between bacteria and resin is relatively less extensive, and CFRP thus exhibits less antibacterial activity than bare resin. The antibacterial properties derived from the vitrimer matrix suggest that it could be used in various fields where antibacterial properties are required, such as medical, water treatment, and coating applications.

4. Conclusion

A carbon fiber-reinforced plastics prepared with vitrimers containing imine groups were characterized. The malleability displayed by the vitrimer with increasing temperature was attributed to the reversible exchange of imine bonds along the polymer chain, as confirmed by stress relaxation experiments. Temperature-dependent behavior of the resins was also observed in reshaping and shape memory experiments. Although the vitrimer composites had weak interfacial bond strength between the vitrimer and carbon fiber, and displayed low interlaminar shear stress, they had tensile strength similar to the reference material. Thus, vitrimer properties had little effect on mechanical performance. Finally, the imine groups along the vitrimer backbone affected the antibacterial properties of its composites with carbon fiber. The antibacterial activity of the vitrimer composites against *S. aureus* was 84.9%, compared with 71.5% for the composites, and both the vitrimer and composites displayed significantly improved antibacterial activity compared with the reference materials lacking imine groups. We concluded that the imine group had a significant positive effect on antibacterial performance in resin and CFRP as well.

Author contribution statement

Wonbin Kim, Yong Min Kim: Performed the experiments; Wrote the paper.
SeungHyeon Song, Eunjung Kim: Performed the experiments; Analyzed and interpreted the data.
Dong-Gyun Kim, Woong-Ryeol Yu: Conceived and designed the experiments.
Yong Chae Jung: Contributed reagents, materials, analysis tools or data.
Wonjin Na: Conceived and designed the experiments; Wrote the paper.
Yong-Seok Choi: Conceived and designed the experiments; Performed the experiments; Analyzed and interpreted the data; Wrote the paper.

Data availability statement

Data included in article/supp. Material/referenced in article.

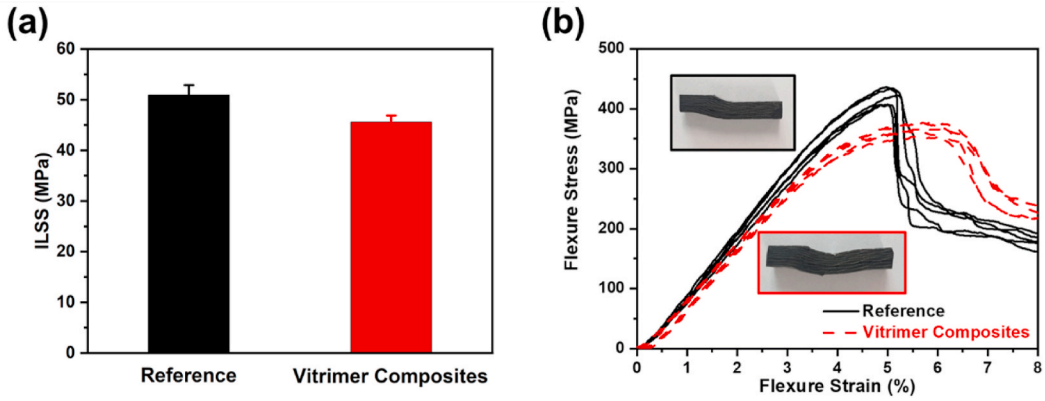

Fig. 7. (A) ILSS of reference and vitrimer composites and (b) comparison of the stress-strain curves.

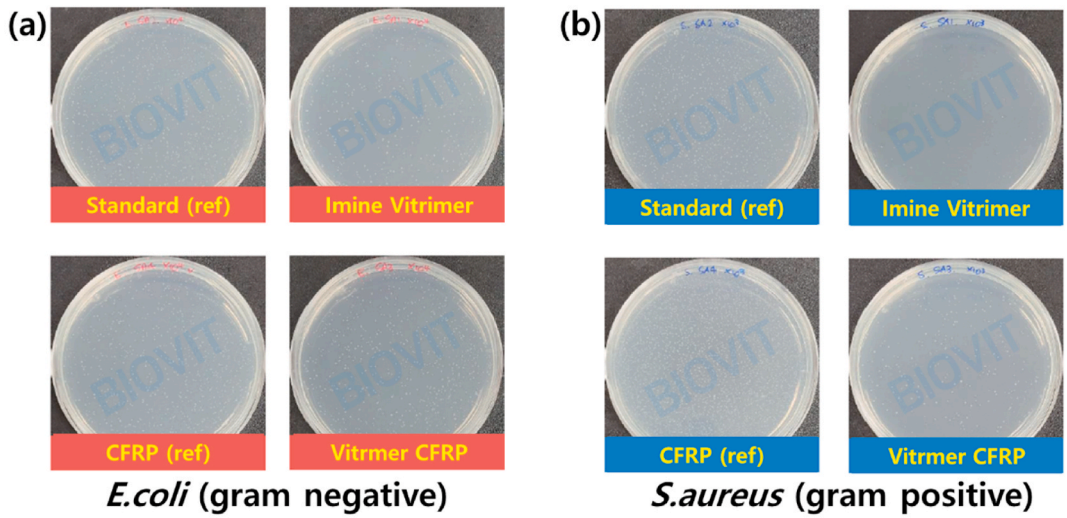

(c)

	Epoxy		Composite	
	Reference	Imine vitrimer	Reference	Imine vitrimer
E.coli	standard	67.9%	-6.0%	-38.9%
S.aureus	standard	84.9%	-13.1%	71.5%

Fig. 8. The antibacterial property of epoxy resin and composites samples against (a) *E. coli*; (b) *S. aureus*; and (c) summary of the antibacterial test.

Declaration of competing interest

The authors declare that they have no known competing financial interests or personal relationships that could have appeared to influence the work reported in this paper.

Acknowledgment

This research was supported by National R&D Program through the institution of South Korea funded by Ministry of Science and ICT (2021M3H4A1A03041296) and by the Jeonbuk Institute for Food-Bioindustry funded by the Regionally Balanced New Deal

Project of the Ministry of the Interior and Safety and Jeollabuk-do. This work was supported by the Technology Innovation Program (20010735, Development of 1 m/min level high speed injection pultrusion materials and process for continuous production of carbon fiber based lightweight car body part and its localization) funded By the Ministry of Trade, Industry & Energy (MOTIE, Korea). The authors are grateful to Biovit Co.,Ltd. For analysis of antibacterial activity.

Appendix A. Supplementary data

Supplementary data to this article can be found online at https://doi.org/10.1016/j.heliyon.2023.e16945.

References

[1] H. Memon, Y. Wei, L. Zhang, Q. Jiang, W. Liu, An imine-containing epoxy vitrimer with versatile recyclability and its application in fully recyclable carbon fiber reinforced composites, Compos. Sci. Technol. 199 (2020), 108314.
[2] S.-J. Park, B.-J. Kim, Carbon fibers and their composites, in: Carbon Fibers, Springer, 2015, pp. 275–317.
[3] C. Barile, C. Casavola, F. De Cillis, Mechanical comparison of new composite materials for aerospace applications, Compos. B Eng. 162 (2019) 122–128.
[4] C.Y.X. Chua, H.-C. Liu, N. Di Trani, A. Susnjar, J. Ho, G. Scorrano, et al., Carbon fiber reinforced polymers for implantable medical devices, Biomaterials 271 (2021), 120719.
[5] N. Forintos, T. Czigany, Multifunctional application of carbon fiber reinforced polymer composites: electrical properties of the reinforcing carbon fibers–A short review, Compos. B Eng. 162 (2019) 331–343.
[6] X. Zheng, S. Kim, C.W. Park, Enhancement of thermal conductivity of carbon fiber-reinforced polymer composite with copper and boron nitride particles, Compos. Appl. Sci. Manuf. 121 (2019) 449–456.
[7] C. Monteserín, M. Blanco, N. Murillo, A. Pérez-Márquez, J. Maudes, J. Gayoso, et al., Novel antibacterial and toughened carbon-fibre/epoxy composites by the incorporation of TiO2 nanoparticles modified electrospun nanofibre veils, Polymers 11 (9) (2019) 1524.
[8] S.J. Lee, I.S. Chung, Optimal design of sandwich composite cradle for computed tomography instrument by analyzing the structural performance and X-ray transmission rate, Materials 12 (2) (2019) 286.
[9] R. Hajj, A. Duval, S. Dhers, L. Avérous, Network design to control polyimine vitrimer properties: physical versus chemical approach, Macromolecules 53 (10) (2020) 3796–3805.
[10] S.-S. Yao, F.-L. Jin, K.Y. Rhee, D. Hui, S.-J. Park, Recent advances in carbon-fiber-reinforced thermoplastic composites: a review, Compos. B Eng. 142 (2018) 241–250.
[11] Y. Tao, L. Fang, M. Dai, C. Wang, J. Sun, Q. Fang, Sustainable alternative to bisphenol A epoxy resin: high-performance recyclable epoxy vitrimers derived from protocatechuic acid, Polym. Chem. 11 (27) (2020) 4500–4506.
[12] S. Wang, S. Ma, Q. Li, X. Xu, B. Wang, K. Huang, et al., Facile preparation of polyimine vitrimers with enhanced creep resistance and thermal and mechanical properties via metal coordination, Macromolecules 53 (8) (2020) 2919–2931.
[13] I. Aranberri, M. Landa, E. Elorza, A.M. Salaberria, A. Rekondo, Thermoformable and recyclable CFRP pultruded profile manufactured from an epoxy vitrimer, Polym. Test. 93 (2021), 106931.
[14] H. Si, L. Zhou, Y. Wu, L. Song, M. Kang, X. Zhao, et al., Rapidly reprocessable, degradable epoxy vitrimer and recyclable carbon fiber reinforced thermoset composites relied on high contents of exchangeable aromatic disulfide crosslinks, Compos. B Eng. 199 (2020), 108278.
[15] D. Montarnal, M. Capelot, F. Tournilhac, L. Leibler, Silica-like malleable materials from permanent organic networks, Science 334 (6058) (2011) 965–968.
[16] B. Krishnakumar, R.P. Sanka, W.H. Binder, V. Parthasarthy, S. Rana, N. Karak, Vitrimers: associative dynamic covalent adaptive networks in thermoset polymers, Chem. Eng. J. 385 (2020), 123820.
[17] R.L. Snyder, D.J. Fortman, G.X. De Hoe, M.A. Hillmyer, W.R. Dichtel, Reprocessable acid-degradable polycarbonate vitrimers, Macromolecules 51 (2) (2018) 389–397.
[18] S. Dhers, G. Vantomme, L. Avérous, A fully bio-based polyimine vitrimer derived from fructose, Green Chem. 21 (7) (2019) 1596–1601.
[19] T.X. Wang, H.M. Chen, A.V. Salvekar, J. Lim, Y. Chen, R. Xiao, et al., Vitrimer-like shape memory polymers: characterization and applications in reshaping and manufacturing, Polymers 12 (10) (2020) 2330.
[20] Z. Yang, Q. Wang, T. Wang, Dual-triggered and thermally reconfigurable shape memory graphene-vitrimer composites, ACS Appl. Mater. Interfaces 8 (33) (2016) 21691–21699.
[21] R. Amin, B. Krammer, N. Abdel-Kader, T. Verwanger, A. El-Ansary, Antibacterial effect of some benzopyrone derivatives, Eur. J. Med. Chem. 45 (1) (2010) 372–378.
[22] R. Fioravanti, M. Biava, G. Porretta, C. Landolfi, N. Simonetti, A. Villa, et al., Research on antibacterial and antifungal agents. XI. Synthesis and antimicrobial activity of N-heteroaryl benzylamines and their Schiff bases, Eur. J. Med. Chem. 30 (2) (1995) 123–132.
[23] A.H. El-masry, H. Fahmy, S. Ali Abdelwahed, Synthesis and antimicrobial activity of some new benzimidazole derivatives, Molecules 5 (12) (2000) 1429–1438.
[24] F. Siedenbiedel, J.C. Tiller, Antimicrobial polymers in solution and on surfaces: overview and functional principles, Polymers 4 (1) (2012) 46–71.
[25] R. Mo, L. Song, J. Hu, X. Sheng, X. Zhang, An acid-degradable biobased epoxy-imine adaptable network polymer for the fabrication of responsive structural color film, Polym. Chem. 11 (5) (2020) 974–981.
[26] W.G. Penney, The theory of the stability of the benzene ring and related compounds, Proc. R. Soc. Lond. - Ser. A Contain. Pap. a Math. Phys. Character 146 (856) (1934) 223–238.
[27] V.V. Krongauz, Crosslink density dependence of polymer degradation kinetics: photocrosslinked acrylates, Thermochim. Acta 503 (2010) 70–84.
[28] Y. Xiong, Z. Jiang, Y. Xie, X. Zhang, W. Xu, Development of a DOPO-containing melamine epoxy hardeners and its thermal and flame-retardant properties of cured products, J. Appl. Polym. Sci. 127 (6) (2013) 4352–4358.
[29] C.S. Wu, Y.L. Liu, Y.S. Chiu, Epoxy resins possessing flame retardant elements from silicon incorporated epoxy compounds cured with phosphorus or nitrogen containing curing agents, Polymer 43 (15) (2002) 4277–4284.
[30] X. Wang, Q. Zhang, Synthesis, characterization, and cure properties of phosphorus-containing epoxy resins for flame retardance, Eur. Polym. J. 40 (2) (2004) 385–395.
[31] J. Zhang, X. Mi, S. Chen, Z. Xu, D. Zhang, M. Miao, et al., A bio-based hyperbranched flame retardant for epoxy resins, Chem. Eng. J. 381 (2020), 122719.
[32] A. Takahashi, T. Ohishi, R. Goseki, H. Otsuka, Degradable epoxy resins prepared from diepoxide monomer with dynamic covalent disulfide linkage, Polymer 82 (2016) 319–326.
[33] Y.-Y. Liu, G.-L. Liu, Y.-D. Li, Y. Weng, J.-B. Zeng, Biobased high-performance epoxy vitrimer with UV shielding for recyclable carbon fiber reinforced composites, ACS Sustain. Chem. Eng. 9 (12) (2021) 4638–4647.
[34] Y. Liu, Z. Tang, J. Chen, J. Xiong, D. Wang, S. Wang, et al., Tuning the mechanical and dynamic properties of imine bond crosslinked elastomeric vitrimers by manipulating the crosslinking degree, Polym. Chem. 11 (7) (2020) 1348–1355.
[35] L. Zhong, Y. Hao, J. Zhang, F. Wei, T. Li, M. Miao, et al., Closed-loop recyclable fully bio-based epoxy vitrimers from ferulic acid-derived hyperbranched epoxy resin, Macromolecules 55 (2) (2022) 595–607.

[36] M. Hayashi, A. Katayama, Preparation of colorless, highly transparent, epoxy-based vitrimers by the thiol-epoxy click reaction and evaluation of their shape-memory properties, ACS Appl. Polym. Mater. 2 (6) (2020) 2452–2457.
[37] W. Na, G. Lee, M. Sung, H.N. Han, W.-R. Yu, Prediction of the tensile strength of unidirectional carbon fiber composites considering the interfacial shear strength, Compos. Struct. 168 (2017) 92–103.
[38] W. Na, D. Kwon, W.-R. Yu, X-ray computed tomography observation of multiple fiber fracture in unidirectional CFRP under tensile loading, Compos. Struct. 188 (2018) 39–47.
[39] S. Wang, Z. Zhou, J. Zhang, G. Fang, Y. Wang, Effect of temperature on bending behavior of woven fabric-reinforced PPS-based composites, J. Mater. Sci. 52 (24) (2017) 13966–13976.
[40] Y. Wang, S.K. Raman Pillai, J. Che, M.B. Chan-Park, High interlaminar shear strength enhancement of carbon fiber/epoxy composite through fiber- and matrix-anchored carbon nanotube networks, ACS Appl. Mater. Interfaces 9 (10) (2017) 8960–8966.
[41] S.P. Sharma, S.C. Lakkad, Comparative study of the effect of fiber surface treatments on the flexural and interlaminar shear strength of carbon fiber-reinforced composites, Mater. Today Commun. (2020) 24.
[42] R. Xie, A.R. Weisen, Y. Lee, M.A. Aplan, A.M. Fenton, A.E. Masucci, et al., Glass transition temperature from the chemical structure of conjugated polymers, Nat. Commun. 11 (1) (2020) 893.
[43] V. Khatkar, B.K. Behera, R.N. Manjunath, Textile structural composites for automotive leaf spring application, Compos. B Eng. (2020) 182.
[44] M. Dahale, G. Neale, R. Lupicini, L. Cascone, C. McGarrigle, J. Kelly, et al., Effect of weave parameters on the mechanical properties of 3D woven glass composites, Compos. Struct. 223 (2019).
[45] S.A. Matar, W.H. Talib, M.S. Mustafa, M.S. Mubarak, M.A. AlDamen, Synthesis, characterization, and antimicrobial activity of Schiff bases derived from benzaldehydes and 3, 3′-diaminodipropylamine, Arab. J. Chem. 8 (6) (2015) 850–857.
[46] X. Xu, S. Ma, J. Wu, J. Yang, B. Wang, S. Wang, et al., High-performance, command-degradable, antibacterial Schiff base epoxy thermosets: synthesis and properties, J. Mater. Chem. 7 (25) (2019) 15420–15431.
[47] H. Oveisi, S. Rahighi, X. Jiang, Y. Nemoto, A. Beitollahi, S. Wakatsuki, et al., Unusual antibacterial property of mesoporous titania films: drastic improvement by controlling surface area and crystallinity, Chem.–Asian J. 5 (9) (2010) 1978–1983.
[48] P. Appendini, J.H. Hotchkiss, Review of antimicrobial food packaging, Innovat. Food Sci. Emerg. Technol. 3 (2) (2002) 113–126.